Extended Abstracts of the 2019 International Conference on Solid State Devices and Materials, Nagoya, 2019, pp837-838

Fabrication and stability characterization of $PbI_2/PbCl_2$ added $CH_3NH_3PbI_{3-x}Cl_x$ solar cells

Naoki Ueoka and Takeo Oku

The University of Shiga Prefecture
2500 Hassaka, Hikone, Shiga 522-8533, Japan
Phone: +81-749-28-8369 E-mail: oh21nueoka@ec.usp.ac.jp

Abstract

The stabilities of $TiO_2/CH_3NH_3PbI_{3-x}Cl_x$ based photovoltaic devices in ambient air were evaluated upon adding PbI_2 and/or $PbCl_2$. X-ray diffraction (XRD) peak intensities corresponding to the perovskite phase were increased by adding PbI_2. After 7 weeks, the XRD peak intensities decreased and those corresponding to PbI_2 increased. Thermodynamic calculations of the reaction between $PbCl_2$ and I_2 suggested that the formation of PbI_2 was not related to the added $PbCl_2$ but rather to excess PbI_2.

1. Introduction

$CH_3NH_3PbI_{3-x}Cl_x$ cells was improved by PbI_2 addition that 10% concentration of 0.8M $PbCl_2$ to the $CH_3NH_3PbI_{3-x}Cl_x$ precursor solution [1]. The recombination of electrons and holes were suppressed by PbI_2 formation and external quantum efficiencies were increased. As a result, the open-circuit voltage (V_{OC}) and short-circuit current density (J_{SC}) were improved. Another previous report agreed that excess PbI_2 in the perovskite layer improved the device efficiency [2]. However, the stability and decomposition mechanisms of $CH_3NH_3PbI_{3-x}Cl_x$ compounds are currently unclear.

The purpose of the present study is to investigate the stability and decomposition mechanism of $CH_3NH_3PbI_{3-x}Cl_x$ solar cells upon adding PbI_2 and/or $PbCl_2$. The carrier transport properties influenced by Pb^{2+} were analyzed.

2. Experimental

J–V characteristics of the photovoltaic cells were measured under illumination at 100 mW cm^{-2}, using an AM 1.5 solar simulator (San-ei Electric, XES-301S). *J–V* measurements were performed using a source measurement unit (Keysight, B2901A Precision SMU). The scan rate and sampling time were ~0.08 V s^{-1} and 1 ms, respectively. Four cells were tested for each cell composition and reported values are averages of these four measurements (η_{ave}). The solar cells were illuminated through the sides of the FTO substrates and the illuminated area was 0.090 cm^2. The microstructures of the cells were investigated using X-ray diffraction (Bruker, D2 PHASER) and scanning electron microscopy (Jeol, JSM-6010PLUS/LA) equipped with EDS. Thermodynamic calculations of the reactions were performed by HSC Chemistry 5 (Outokumpu Research Oy). Fig. 1 shows the schematic illustration of the perovskite photovoltaic device.

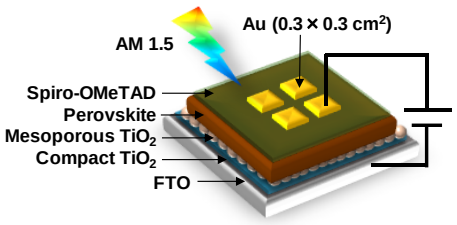

Perovskite precursor solution

Cells	CH_3NH_3I : $PbCl_2$	PbI_2	$PbCl_2$
Standard	2.4 M : 0.8 M		
+ PbI_2	2.4 M : 0.8 M	0.08 M	
+ PbI_2 + $PbCl_2$	2.4 M : 0.8 M	0.08 M	0.05 M
+ PbI_2 (HC)	2.7 M : 0.9 M	0.08 M	

Fig. 1. Schematic illustration of the perovskite photovoltaic device.

3. Results and discussion

The Gibbs free energy (ΔG) of the reactions were calculated and the results are shown in Fig. 2. The ΔG values for the formation of PbI_2 from Pb + I_2 and $PbCl_2$ + I_2 at room temperature were negative and positive, respectively, which indicated that PbI_2 formed from Pb + I_2. These results indicated that the formation of PbI_2 was not due to excess $PbCl_2$

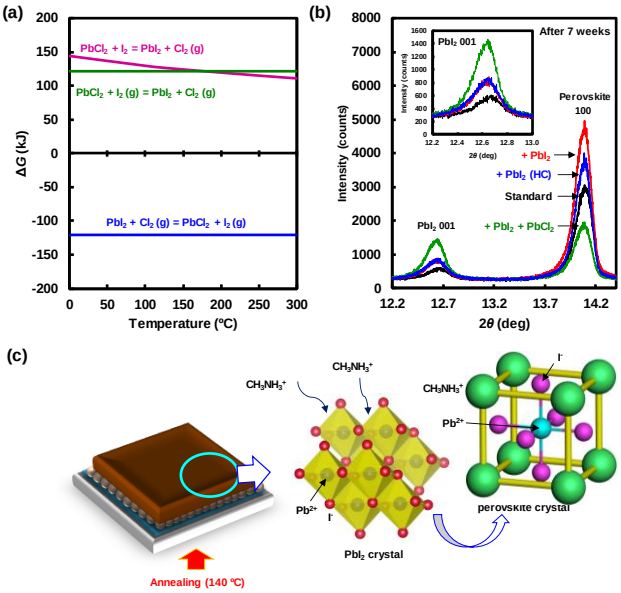

Fig. 2. (a) Thermodynamic calculations of the ΔG for the reaction, (b) XRD patterns after 7 weeks and (c) schematic illustrations of formation mechanism of perovskite crystal.

but to excess PbI_2 or the decomposition of $CH_3NH_3PbI_{3-x}Cl_x$ perovskite grains. The diffraction peaks of the + PbI_2 (HC) cell were similar to those of the + PbI_2 cell. For the same quantity of added PbI_2, the separation of PbI_2 crystals did not depend on the concentration of the perovskite precursor solution, as shown in Fig. 2 (b). PbI_2 crystals were formed at 90℃ [3], and the perovskite crystals were formed by reaction of $CH_3NH_3^+$ and PbI_2, as shown in Fig. 2 (c).

Normalized intensities of the 100 diffraction peaks of perovskite and 001 diffraction peaks of PbI_2 are shown in Fig. 3 (a) and (b), respectively. Average reaction rate constants for the decomposition of perovskite crystals (k_1) and the formation of PbI_2 (k_2) were estimated from the diffraction intensities and are summarized in Table 1. The k_1 value for the + PbI_2 cell was the smallest among the present devices, which indicated that the decomposition of perovskite grains was suppressed by the PbI_2 crystals. The k_1 and k_2 values for the + PbI_2 + $PbCl_2$ cell were the highest and lowest, respectively, which indicated that the perovskite grains decomposed upon adding excess PbI_2. The most ratio of PbI_2 formation of + PbI_2 + $PbCl_2$ cell for the decomposition of perovskite crystals.

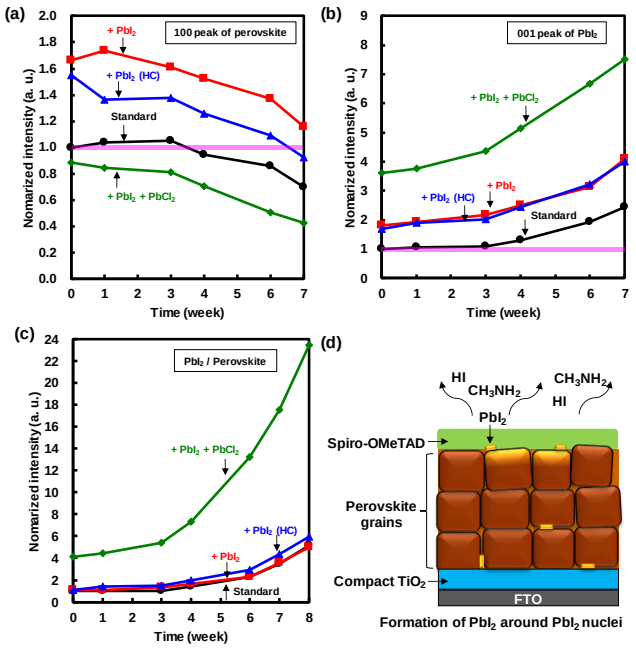

Fig. 3. Normalized XRD intensities of the (a) 100 peak of perovskite, (b) 001 peak of PbI_2, (c) PbI_2/perovskite and (d) schematic illustration of decomposition mechanism for the perovskite photovoltaic devices, respectively.

Table 1. Reaction rate constants for the decomposition of perovskite crystals (k_1) and formation of PbI_2 (k_2).

Cell	$k_1 \times 10^{-7}$ (s^{-1})	$k_2 \times 10^{-7}$ (s^{-1})
Standard	**1.36**	**2.24**
+ PbI_2	**1.19**	**2.13**
+ PbI_2 + $PbCl_2$	**1.78**	**1.73**
+ PbI_2 (HC)	**1.54**	**2.28**

The formation of PbI_2 was considered to be due to the desorption of CH_3NH_2 and *HI* from the surface of the $CH_3NH_3PbI_{3-x}Cl_x$ perovskite phase, as shown in Fig. 3 (d).

The atomic ratios of Cl/Pb remained almost constant. Once PbI_2 crystals formed around PbI_2 nuclei on the surface of the perovskite, decomposition of the perovskite crystals was suppressed by the added PbI_2 for the + PbI_2 cell. As a result, the conversion efficiency was maintained for 7 weeks for device with added PbI_2, as shown in Fig. 4 (a) and (b). The distribution density of the perovskite grains increased and the smoothness of the perovskite/spiro-OMeTAD interface was increased, which resulted in the increase in V_{OC} and *FF*. Charge transport time would be shorter for the + PbI_2 cell because PbI_2 crystals transport carriers efficiently in the perovskite layer compared with the standard cell [4-5]. Since PbI_2 is a *p*-type semiconductor with the bandgap energies of 2.3~2.6 eV, the PbI_2 could also work as a hole transport layer in the perovskite phase, as shown in Fig. 4 (c) and (d).

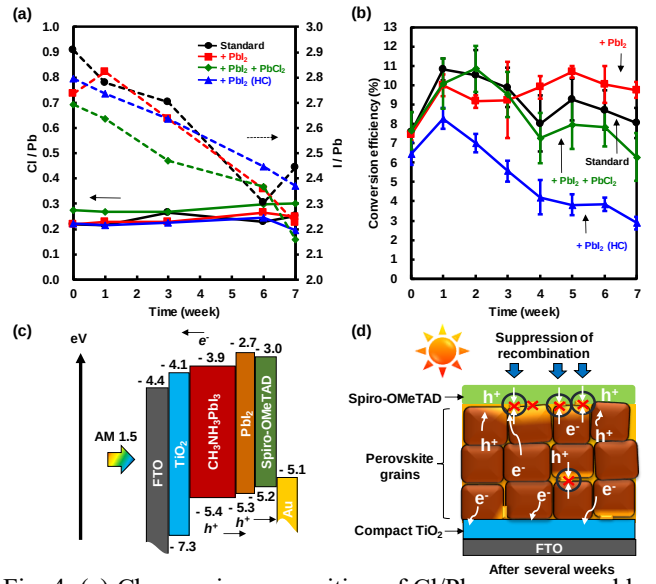

Fig. 4. (a) Changes in composition of Cl/Pb, as measured by EDS, (b) changes in conversion efficiency, (c) energy level diagram and (d) schematic illustration of carrier transport mechanism for the perovskite photovoltaic devices, respectively.

References

1. N. Ueoka, T. Oku, Y. Ohishi, H. Tanaka, and A. Suzuki, Chem. Lett. **47** (2018) 528.
2. V. Kapoor, A. Bashir, L. J. Haur, A. Bruno, S. Shukla, A. Priyadarshi, N. Mathews, and S. Mhaisalkar, Energy Technol. **5** (2017) 1880.
3. A. Wakamiya, M. Endo, T. Sasamori, N. Tokitoh, Y. Ogomi, S. Hayase, and Y. Murata, Chem. Lett. **43** (2014) 711.
4. P. S. Chandrasekhar, A. Dubey, K. M. Reze, M. D. N. Hasan, B. Bahrami, V. K. Komarala, J. D. Hoefelmeyer, Q. He, F. Wu, H. Qiao, W. H. Zhang, and Q. Qiao, Sustainable Energy Fuels **2** (2018) 2260.
5. N. Ueoka and T. Oku, ACS Appl. Mater. Interfaces **10** (2018) 44443.